Available online at www.sciencedirect.com
ScienceDirect
Medical Image Analysis 12 (2008) 514–523
MEDICAL IMAGE ANALYSIS
www.elsevier.com/locate/media

MRI denoising using Non-Local Means

José V. Manjón [a,*], José Carbonell-Caballero [a], Juan J. Lull [a], Gracián García-Martí [a], Luís Martí-Bonmatí [b], Montserrat Robles [a]

[a] *Biomedical Informatics Group (IBIME), ITACA Institute, Polytechnic University of Valencia, Camino de Vera, s/n. 46022 Valencia, Spain*
[b] *Department of Radiology, Dr. Peset Hospital and Quirón Hospital, Valencia, Spain*

Received 30 October 2006; received in revised form 12 February 2008; accepted 13 February 2008
Available online 29 February 2008

Abstract

Magnetic Resonance (MR) images are affected by random noise which limits the accuracy of any quantitative measurements from the data. In the present work, a recently proposed filter for random noise removal is analyzed and adapted to reduce this noise in MR magnitude images. This parametric filter, named Non-Local Means (NLM), is highly dependent on the setting of its parameters. The aim of this paper is to find the optimal parameter selection for MR magnitude image denoising. For this purpose, experiments have been conducted to find the optimum parameters for different noise levels. Besides, the filter has been adapted to fit with specific characteristics of the noise in MR magnitude images (i.e. Rician noise). From the results over synthetic and real images we can conclude that this filter can be successfully used for automatic MR image denoising.

Keywords: MRI filtering; Random noise; Denoising

1. Introduction

Magnetic Resonance (MR) images are affected by several artifacts and noise sources. One of them is the random fluctuation of the MR signal which is mainly due to thermal noise. Such a noise seriously degrades the acquisition of any quantitative measurements from the data (especially functional MR imaging [fMRI] is very sensitive to the noise level since BOLD signal variations are in the same range).

Although random noise can be naturally minimized by increasing the Number of Signal Averages (NSA) during the acquisition of the MR images (Gerig et al., 1992), this may not be a suitable alternative in clinical MR imaging where there is an increasing *need for speed*.

The removal of noise from noisy data to obtain the unknown signal is often referred to as denoising. Postprocessing filtering techniques have the advantage of not to increase the acquisition time and, therefore, they have been extensively used in MRI denoising. Most denoising methods are based on the signal averaging principle by using the spatial pattern redundancy in the image. However, there are other filtering techniques that use other statistical estimates such us the median (Ling and Bovik, 2002; Liévin et al., 2002). Gaussian filters have been largely used in some applications such as fMRI (Ashburner and Friston, 2000) but they have the disadvantage of blurring edges by averaging pixels with non-similar patterns. In order to avoid such problem many edge preserving filters, like the Anisotropic Diffusion Filter (ADF) (Perona and Malik, 1990; Gerig

Abbreviations: NLM, Non-Local Means; UNLM, Unbiased Non-Local Means; BOLD, Blood Oxygen Level Dependent; ADF, Anisotropic Diffusion Filter; NSA, Number of Signal Averages; TV, Total Variation; RMSE, Root Mean Square Error; SNR, Signal to Noise Ratio.

* Corresponding author. Tel.: +34 96 387 70 00x75275; fax: +34 96 387 90 09.
E-mail addresses: jmanjon@fis.upv.es (J.V. Manjón), jocarca1@itaca.upv.es (J. Carbonell-Caballero), jualulno@upv.es (J.J. Lull), gragarma@fis.upv.es (G. García-Martí), luis.marti@uv.es (L. Martí-Bonmatí), mrobles@fis.upv.es (M. Robles).

1361-8415/$ - see front matter © 2008 Elsevier B.V. All rights reserved.
doi:10.1016/j.media.2008.02.004

et al., 1992; Samsonov and Johnson, 2004) have been used. Such filters respect edges by averaging pixels in the orthogonal direction of the local gradient. However, such filtering usually erases small features and transforms image statistics due to its edge enhancement effect resulting in an unnatural image.

Modern wavelet-based filters have been also applied to MRI denoising (Nowak, 1999; Wood and Johnson, 1999; Pizurica et al., 2003) but such filters may introduce characteristic artifacts that can be quite problematic. More recently, the trilateral filter (Wong and Chung, 2004), an evolution of the bilateral filter (Tomasi and Manduchi, 1998), has been proposed to take into account local structure in addition to intensity and geometric features.

Our objective was to study and improve the application of a new filter, recently proposed by Buades et al. (2005) to denoise magnitude MR images. This filter is named Non-Local Means (NLM). In the comparative provided by the authors, it is shown that this method outperforms clearly other classic methods like ADF, Total Variation (TV) (Rudin et al., 1992) or wavelet thresholding methods (Coifman and Donoho, 1995) among others.

2. Materials and methods

2.1. The NLM filter

The NLM filter is an evolution of the Yaroslavsky filter (Yaroslavsky, 1985) which averages similar image pixels according to their intensity distance. Some filters, like the SUSAN (Smith and Brady, 1997) or the bilateral filters are based in the same principle. The main differences of the NLM with these methods is that the similarity between pixels is more robust in front of the noise level by using region comparison rather than pixel comparison and that pattern redundancy is not restricted to be local (therefore, non-local). Pixels far from the pixel being filtered are not penalized due to its distance to the current pixel, as happens with the bilateral filter.

Let us introduce the description of the NLM filter.

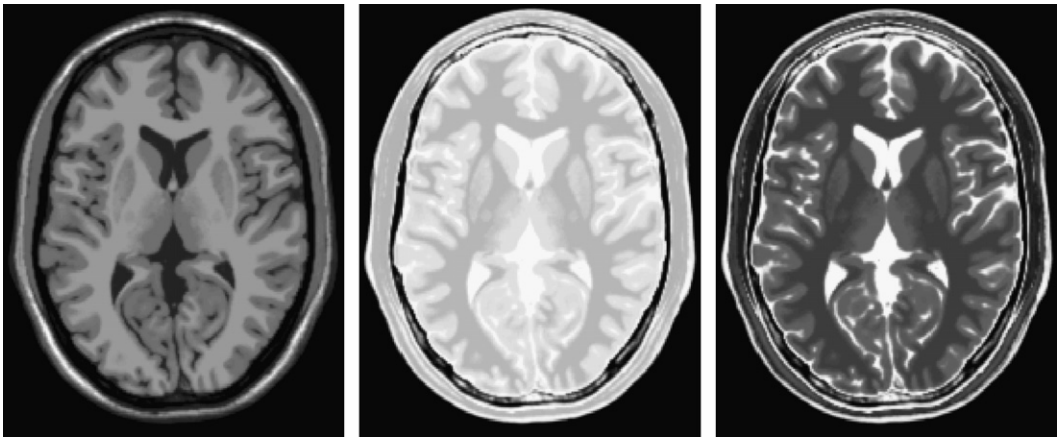

Fig. 1. Simulated MR images (T1, PD and T2) from the Brainweb phantom.

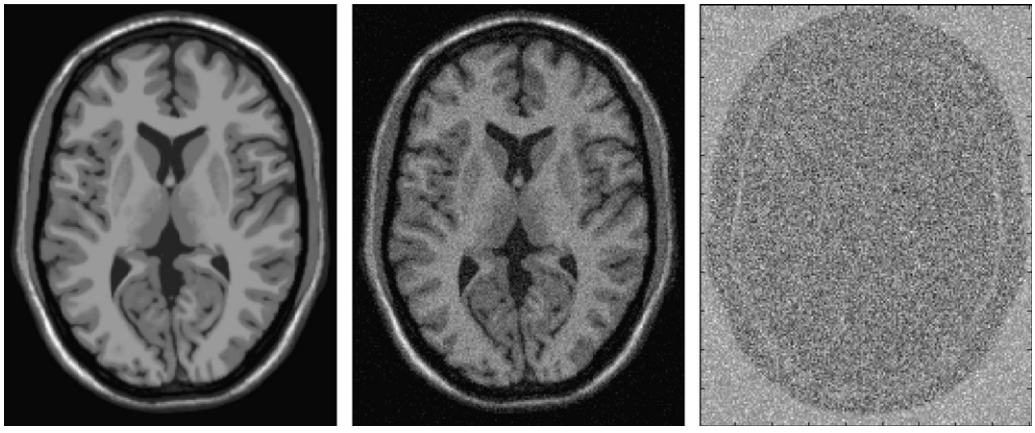

Fig. 2. From left to right: T1-weighted synthetic noise-free MR image, the corresponding noisy image ($\sigma = 12$) and the applied noise (difference between both images). Note that the background pixels have a higher value than the foreground due to the Rician bias.

Given an image Y, the filtered value at a point p using the NLM method is calculated as a weighted average of all the pixels in the image following this formula:

$$\mathrm{NLM}(Y(p)) = \sum_{\forall q \in Y} w(p,q) Y(q)$$
$$0 \leqslant w(p,q) \leqslant 1 \quad \sum_{\forall q \in Y} w(p,q) = 1 \tag{1}$$

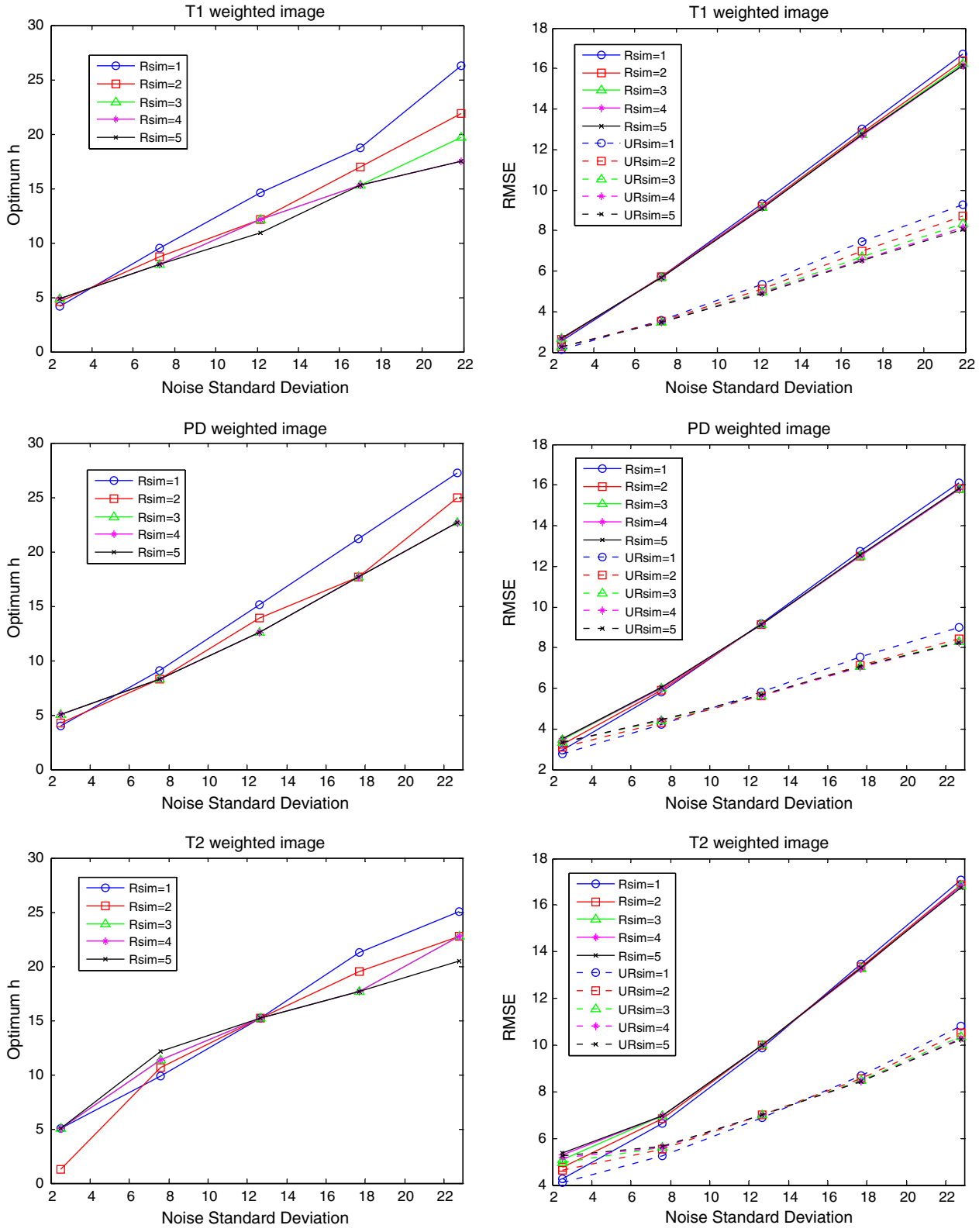

Fig. 3. Left: optimum h values for different noise levels and different radius of the similarity window. Right: RMSE for different noise levels and different values of radius of the similarity window. Dotted lines represent the results of the unbiased NLM filter.

Table 1
Optimal h values for different types of MR images and different values of R_{sim} parameter ($R_{search} = 5$)

R_{sim}		1	2	3	4	5
Optimal h	T1	1.30σ	1.22σ	1.18σ	1.18σ	1.14σ
	PD	1.26σ	1.18σ	1.14σ	1.14σ	1.11σ
	T2	1.25σ	1.18σ	1.14σ	1.13σ	1.10σ

where p is the point being filtered and q represents each one of the pixels in the image. The weights $w(p,q)$ are based on the similarity between the neighborhoods N_p and N_q of pixels p and q. N_i is defined as a square neighbourhood window centered around pixel i with a user-defined radius R_{sim}. The similarity $w(p,q)$ is then calculated as

$$w(p,q) = \frac{1}{Z(p)} e^{-\frac{d(p,q)}{h^2}} \quad (2)$$

$$Z(p) = \sum_{\forall q} e^{-\frac{d(p,q)}{h^2}} \quad (3)$$

$Z(p)$ is the normalizing constant, h is a exponential decay control parameter and d is a Gaussian weighted Euclidian distance of all the pixels of each neighbourhood:

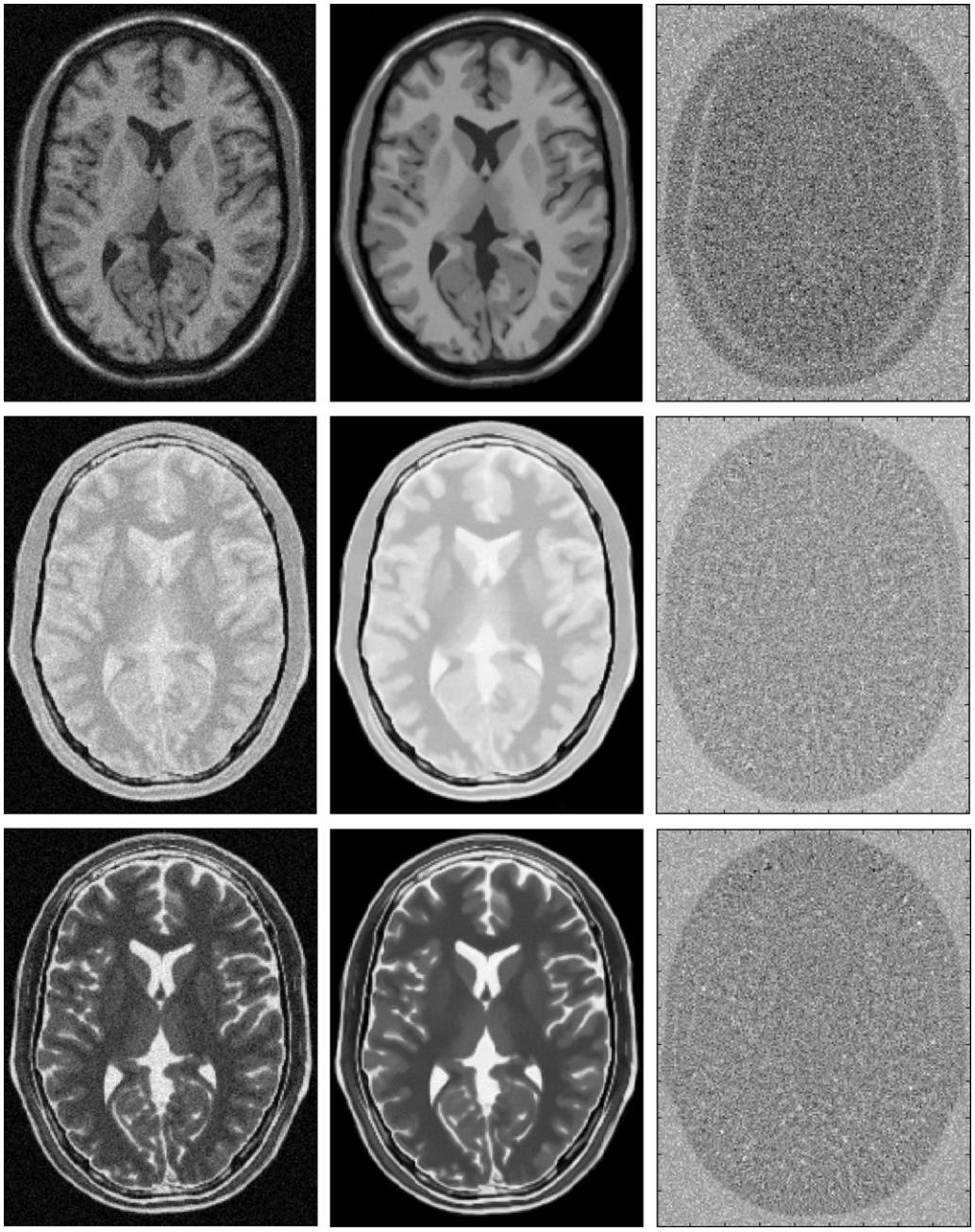

Fig. 4. Top row; from left to right: T1-weighted synthetic noise-free MR image with 5% Rician noise, UNLM filtered image (using the optimum parameters above estimated) and the corresponding residuals. Middle row; and bottom row: same results for a simulated PD-weighted and T2-weighted images. Note that the background pixels have a higher value than the foreground due to Rician bias correction in both cases.

$$d(p,q) = G_\rho \|Y(N_p) - Y(N_q))\|^2_{R_{\text{sim}}} \quad (4)$$

where G_ρ is a normalized Gaussian weighting function with zero mean and ρ standard deviation (usually set to 1) that penalizes pixels far from the center of the neighbourhood window by giving more weight to pixels near the center. The center pixel of the Gaussian weighting window is set to the same value that the pixels at a distance 1 to avoid over-weighting effects.

In Eq. (1) there is a special case when $p = q$. As the self similarity is very high, it can produce an over-weighting effect. To solve this situation $w(p,p)$ is calculated as

$$w(p,p) = \max(w(p,q) \forall q \neq p) \quad (5)$$

2.2. The special nature of the MR magnitude images

As the magnitude of the MRI signal is the square root of the sum of the squares of Gaussian distributed real and imaginary parts, it follows a Rician distribution (Sijbers and den Dekker, 2004). In low intensity regions of the image, the Rician distribution tends to a Rayleigh distribution while in high intensity regions it approaches to a Gaussian distribution. As a result the image contrast is reduced.

It was shown that this problem can be efficiently overcome by filtering the square of the MRI magnitude image (Nowak, 1999). In the squared magnitude image, the noise bias is not longer signal-dependent and it can be easily removed. Such bias is equal to $2\sigma^2$ as shown by Nowak and, therefore, a simple bias subtraction will recover its original value. This value can be estimated as the mean value of the background intensities of the squared noisy image were the signal should be zero.

Thus, the unbiased NLM (UNLM) estimation will be defined as follows:

$$\text{UNLM}(Y) = \sqrt{\text{NLM}(Y)^2 - 2\sigma^2} \quad (6)$$

2.2.1. UNLM – method summary

The proposed method can be summarized as follows:

1. Estimate image noise: this can be done from the image background (Eq. (8)).
2. For every pixel in the image use Eq. (1) to compute the filtered value (optimum filter parameters are describe in the next section).
3. For every pixel in the image calculate the unbiased value by applying Eq. (6).

3. Experiments and results

The NLM algorithm has three parameters and the filter results depend highly on their setting. Let us to describe each one of them.

The first parameter, R_{search}, is the radius of a search window. Although the original method claims to use all the pixels in the image by taking the weighted average of every pixel, it is very inefficient and, therefore, the search window has to be reduced to a window N_p of smaller size:

$$\text{NLM}(Y(p)) = \sum_{\forall q \in N_p} w(p,q) Y(q) \quad (7)$$

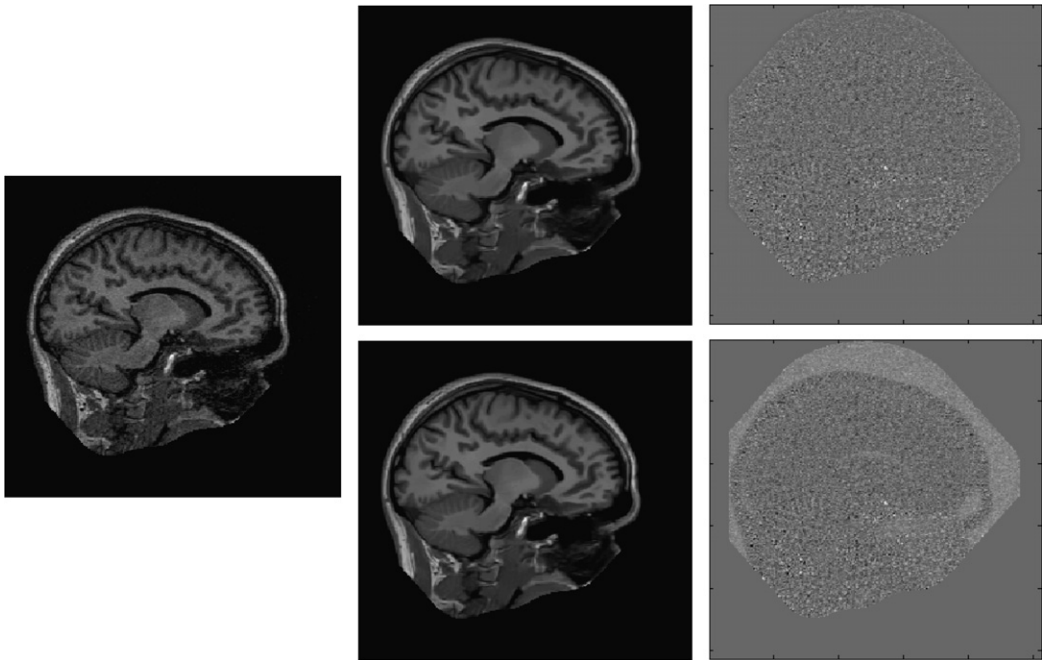

Fig. 5a. Left: noisy T1-weighted image (estimated sigma = 10.2). Center up: results for NLM $(5,2,1.2\sigma)$ and down results for UNLM $(5,2,1.2\sigma)$. At the right, the corresponding image residuals. Note that the background is truncated due the application of a defacer to the dataset.

The second parameter, R_{sim}, is the radius of the neighbourhood window used to find the similarity between two pixels. If the value of R_{sim} is increased the similarity measure will be more robust but fewer similar neighbourhoods will be found.

The third parameter, h, is related to the decay of the exponential curve and controls the degree of smoothing. If h is too small, little noise will be removed while if h is set too high, the image will become blurry.

In our experiments we have set R_{search} to 5 (this is a 11×11 search window), which seems a reasonable value for medical images. The best settings for R_{sim} and h under different noise levels were evaluated as follows.

3.1. Synthetic data

To conduct the experiments over synthetic data 3 simulated MR images (T1, PD and T2) with 1 mm^3 voxel reso-

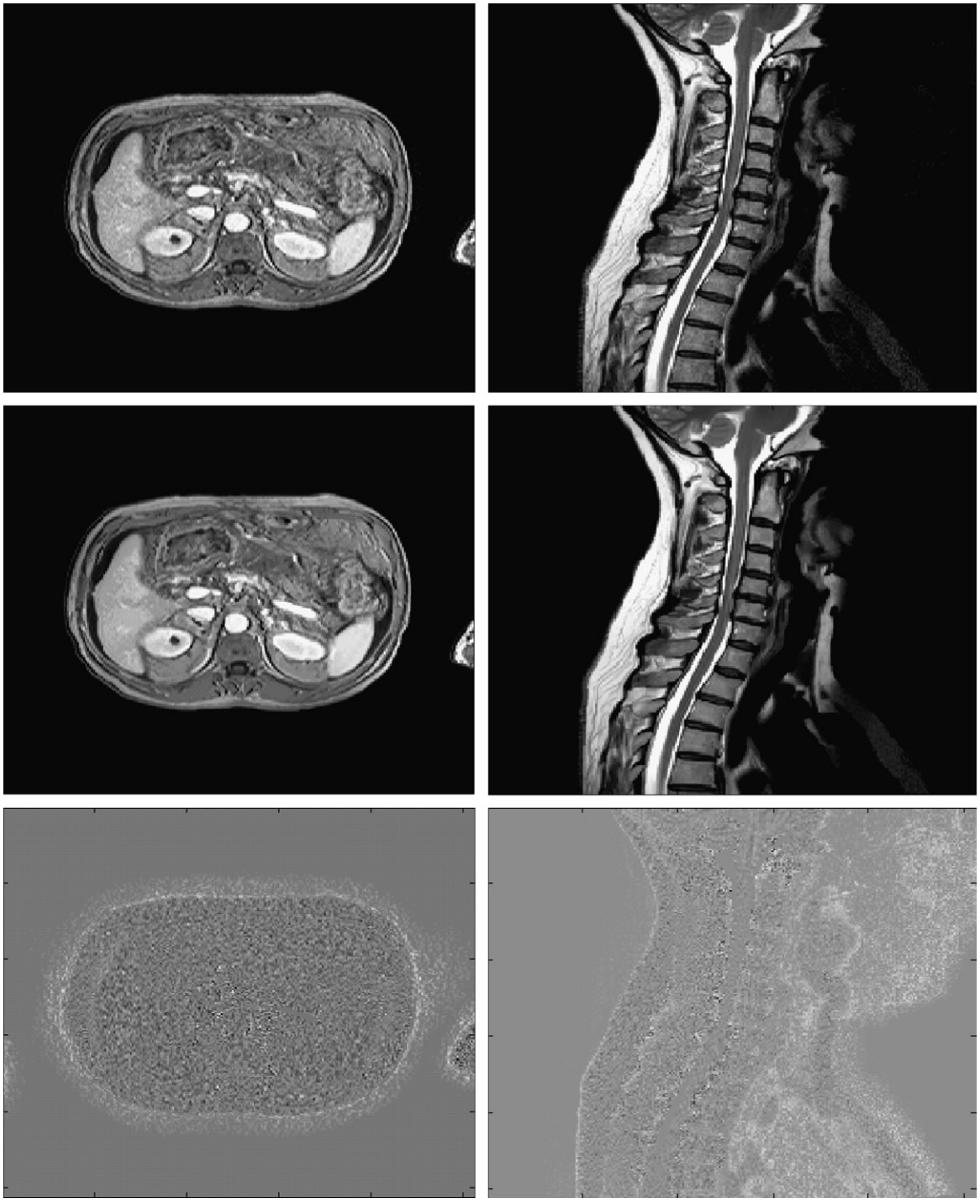

Fig. 5b. Left column: noisy T1-weighted abdominal image, results for UNLM $(5, 2, 1.2\sigma)$ and image residuals. Right column: noisy T2-weighted spine image, results for UNLM $(5, 2, 1.2\sigma)$ and image residuals.

lution (8 bit quantization) from the Brainweb phantom (Cocosco et al., 1997) (Fig. 1) were used. To simulate Rician noise we added zero mean Gaussian noise to the real and imaginary parts of the simulated MR data and afterwards the magnitude image was computed (Fig. 2). All experiments were performed using MATLAB 7.0 (Mathwoks Inc.).

To measure the quality of the filter, the Root Mean Squared Error (RMSE) was used. For each R_{sim} value ($R_{sim} \in [1,5]$) an exhaustive search for the optimum h value (using the RMSE criteria) was performed. Results for different noise levels (1%, 3%, 5%, 7% and 9% of the maximum intensity) and image type can be seen in Fig. 3.

As can be observed, there is a linear relation between noise level and the optimum h value. In Table 1, the optimal h values for different R_{sim} values and image type (in terms of the noise level) are shown. As expected, the RMSE is minimized as R_{sim} increases (Fig. 3). However, as the temporal cost of the filter increased drastically as a function of R_{sim}, a good compromise between accuracy and computational load was found to be $R_{sim} = 2$, since further increasing this value did not produce a noticeable improvement but increased notably the filter temporal cost. From the obtained results over synthetic data we suggest, in a general framework, to use an h value around 1.2σ with $R_{sim} = 2$ and $R_{search} = 5$.

In Fig. 4, an example of filtering results with the proposed parameters for different MR image types can be qualitatively evaluated. Almost no anatomical information can be noticed in the image residuals. The Rician bias correction is also noticeable in the residuals.

3.2. Application to clinical MR data

To test the filter over real data we used two different datasets covering brain and body locations. The first image

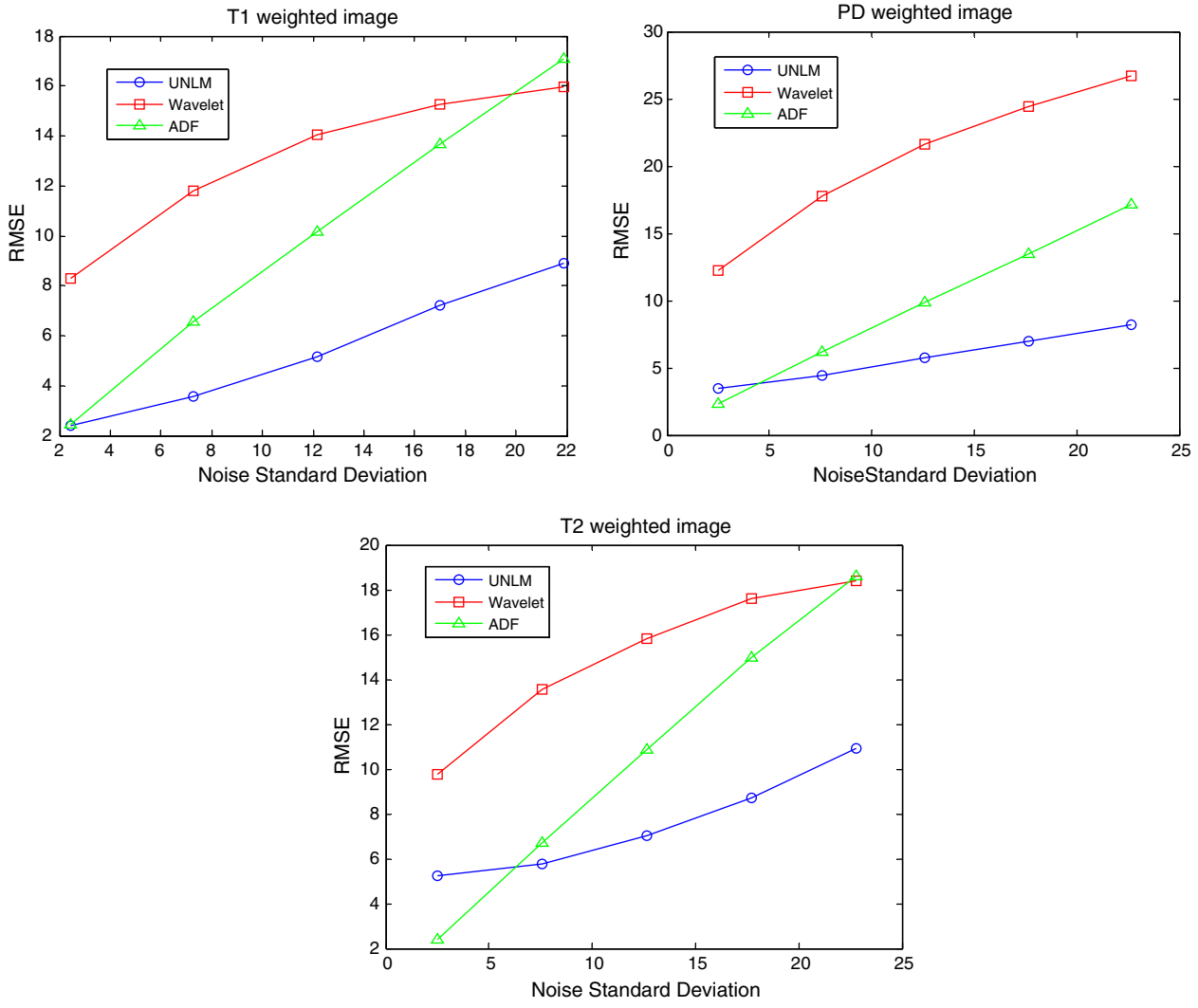

Fig. 6. RMSE comparison of the different filters for different image types and noise conditions. The proposed method outperforms the others in almost all the cases (in terms of RMSE).

was a T1-weighted sagittal MP-RAGE scan acquired on a Siemens 1.5 Tesla Vision scanner (Erlangen, Germany). This data was obtained from the fMRI Data Center database (http://www.fmridc.org/).

The second set was two body images acquired on a Philips 3 Tesla scanner (Achieva, Philips Medical Systems, Best, The Netherlands). This data was obtained from Hospital Quirón of Valencia (Spain).

To apply the UNLM to real magnitude MR images the standard deviation of the complex Gaussian noise σ needs to be estimated. This can be calculated from the background of the squared magnitude image (Nowak, 1999) as follows:

$$\sigma = \sqrt{\frac{\mu}{2}} \tag{8}$$

where μ is the mean value of the background of the squared magnitude image which was selected using an Otsu thresholding method (Otsu, 1979). Example results can be observed in Figs. 4 and 5.

3.3. Method comparative

We have compared, qualitative and quantitatively, the performance of our proposed algorithm (with optimal estimated parameters) with two state-of-the-art filtering

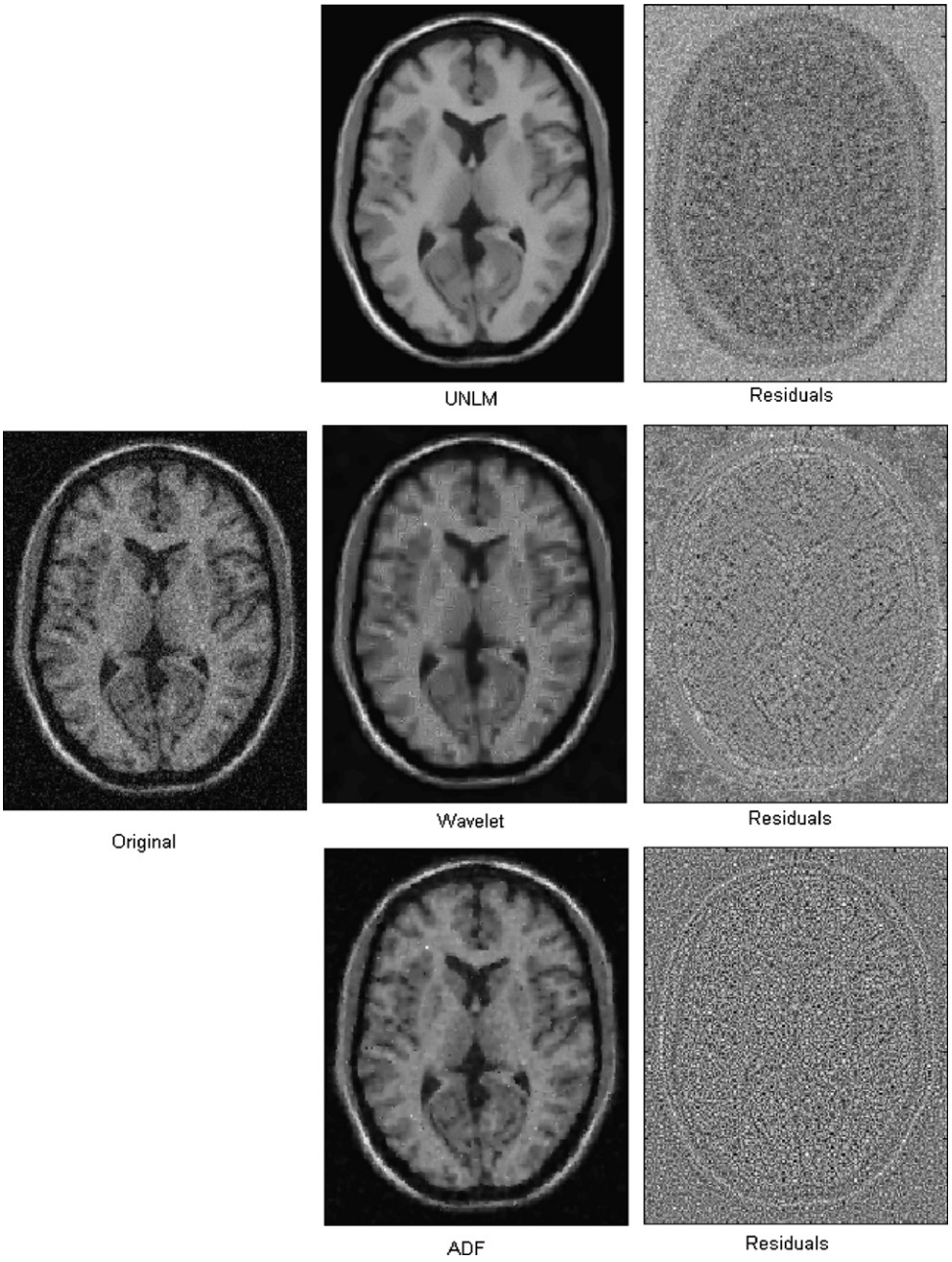

Fig. 7. Qualitative comparison of the filtering results obtained with the different compared methods (9% noise corrupted T1-weighted image). The quality of the proposed filter can be noticed in both filtered image and the corresponding residuals.

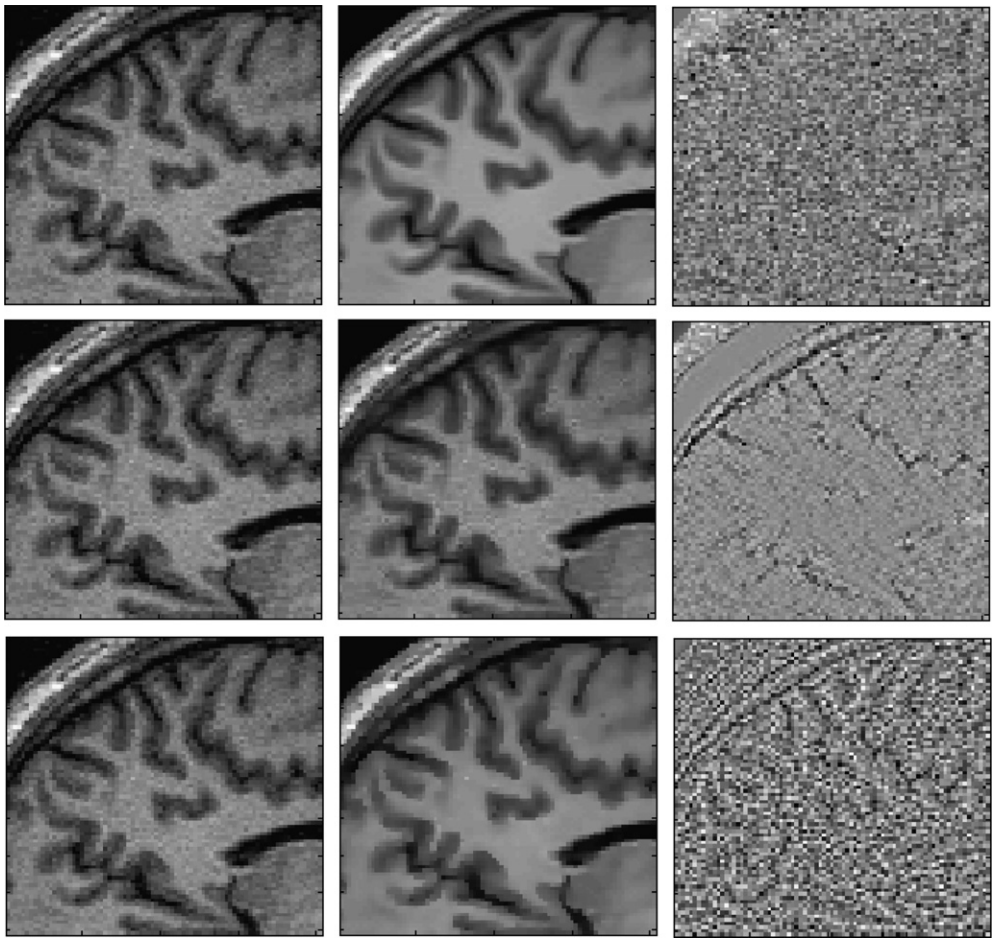

Fig. 8. Qualitative comparison of the filtering results obtained with the different compared methods (close up of a real T1-weighted image with an estimated noise standard deviation of 10.2). From top to down: UNLM, Wavelet and ADF results. From left to right: original image, denoised and the corresponding residuals.

algorithms, the ADF (Perona and Malik, 1990) and a modern wavelet-based denoising algorithm (Pizurica et al., 2003). We have manually tuned all the free parameters of the ADF in order to give the best possible results and we have used the parameters proposed by the authors in the case of wavelet-based denoising.

The proposed algorithm was quantitatively compared, using the synthetic data referred in Section 3.1, with the other two referred methods showing a lower RMSE in almost all the cases (Fig. 6). Besides, the real T1-weighted image of the Section 3.2 was also used to compare the different filters (Fig. 8).

Qualitatively, the proposed algorithm gives a residual (difference between denoised and original image) that is significantly less correlated (Figs. 7 and 8). The ADF shows an unnatural edge enhancement and a blurring of small edges. Finally, the wavelet-based denoising algorithm also seems to introduce artifacts in the denoised image.

4. Conclusion/discussion

We have presented and analyzed the application of the NLM filter for magnitude MR image denoising. This filter can be used to increase the SNR of the MR images without affecting noticeable structures in the image. Proper parameterization of the filter has been studied using an objective criterion (i.e. RMSE). Furthermore, an unbiased version of the filter has been proposed that outperforms the original method in the MRI denoising context.

Although RMSE is a very useful quantitative criterion for evaluating filter performance, it does not guarantee optimal filtering in the visual perception sense. A good filter must extract as much noise as possible from the image while keeping image features unaltered. As there is no objective criteria fully meeting such requirements, visual inspection of the image residuals (i.e. the difference between the original and the filtered image) was also used to evaluate filter efficacy: the so called *method noise* proposed by Buades et al. (2005). According to this criteria, the optimal h value was estimated to be around σ for $R_{\text{sim}} = 2$. As this is a subjective impression we have not conducted our experiments according to this criteria.

It is clear that the extension of the UNLM filter to three-dimensions will further improve the results due to mainly two reasons. First, a 3D neighbourhood will produce a more robust similarity measure than in 2D and, second,

the number of similar patterns surrounding each voxel will be increased. In a similar manner, results can be further improved by using multiple channels (i.e. multispectral imaging) to compute pixel similarities on a more robust way. It is our intention to explore all this issues in a near future.

However, it should be noted that the computational cost of the filter increases notably in 3D. A typical size dataset ($256 \times 256 \times 90$ pixels) takes around 7 min to be filtered with the 2D version of the filter and the proposed parameter settings (using a mex file in Matlab 7.0). A 3D version of this filter will take several hours and the multispectral version will increase this time lineary with the number of channels. An appropriate solution to reduce the computational burden may be the use of a Grid system (Blanquer et al., 2006) since the filter can be easily adapted to work on a parallel system by dividing the volume on small independent volumes. Another possibility to speed up the method is to do a selection of the most similar pixels by using local intensity and gradient features (Mahmoudi and Sapiro, 2005) to avoid neighbourhood distance calculations which are the most time consuming part of the filter.

Finally, it is our aim to improve the filter results using a rotational invariant similarity measure in the region comparison step since presently a rotated similar pattern have a low similarity value. This new similarity measure will increase the number of similar patterns in the search window by taking into account not only structure but also orientation.

Acknowledgements

We want to thank Dr. A. Buades for his useful comments along this project. We want also to thank the Hospital Quirón of Valencia and the fMRI Data Center database (http://www.fmridc.org/) for providing access to the MR data used in this paper. This work has been possible thanks to the IM3 (ISCIII – G03/185) and INBIOMED (ISCIII – G03/160) Spanish research networks. This research was also supported by ADIRM association.

References

Ashburner, J., Friston, K.J., 2000. Voxel-based morphometry – the methods. NeuroImage 11, 805–821.

Blanquer, I., Hernández, V., Monleón, D., Carbonell, J., Moratal, D., Celda, B., Robles, M., Martí-Bonmatí, L., 2006. Using the grid to analyze the pharmacokinetic modelling after contrast administration in dynamic MRI. Studies in Health Technologies and Informatics 120, 82–92.

Buades, A., Coll, B., Morel, J.M., 2005. A review of image denoising algorithms, with a new one. Multiscale Modeling and Simulation 4 (2), 490–530.

Cocosco, C.A., Kollokian, V., Kwan, R.K.-S., Evans, A.C., 1997. BrainWeb: online interface to a 3D MRI simulated brain database. NeuroImage 5 (4).

Coifman, R.R., Donoho, D., 1995. Translation-invariant De-noising, in Wavelets and Statistics. Springer-Verlag, New York, pp. 125–150.

Gerig, G., Kubler, O., Kikinis, R., Jolesz, F.A., 1992. Nonlinear anisotropic filtering of MRI data. IEEE Transactions on Medical Imaging 11, 221–232.

Liévin, M., Luthon, F., Keeve, E., 2002. Entropic estimation of noise for medical volume restoration. Pattern Recognition 3, 871–874.

Ling, J., Bovik, A.C., 2002. Smoothing low-SNR molecular images via anisotropic median-diffusion. IEEE Transactions on Medical Imaging 21 (4), 377–384.

Mahmoudi, M., Sapiro, G., 2005. Fast image and video denoising via nonlocal means of similar neighborhoods. IEEE Signal Processing Letters 12 (12), 839–842.

Nowak, R.D., 1999. Wavelet-based Rician noise removal for magnetic resonance imaging. IEEE Transactions on Image Processing 8 (10), 1408–1419.

Otsu, N., 1979. A threshold selection method from gray-level histograms. IEEE Transactions on Systems, Man and Cybernetics 9 (1), 62–69.

Perona, P., Malik, J., 1990. Scale space and edge detection using anisotropic diffusion. IEEE Transactions on Pattern Analysis and Machine Intelligence 12, 629–639.

Pizurica, A., Philips, W., Lemahieu, I., Acheroy, M., 2003. A versatile wavelet domain noise filtration technique for medical imaging. IEEE Transactions on Medical Imaging 22 (3), 323–331.

Rudin, L., Osher, S., Fatemi, E., 1992. Nonlinear total variation based noise removal algorithms. Physica D 60, 259–268.

Samsonov, A., Johnson, C., 2004. Noise-adaptive nonlinear diffusion filtering of MR images with spatially varying noise levels. Magnetic Resonance in Medicine 52, 798–806.

Sijbers, J., den Dekker, A.J., 2004. Maximum likelihood estimation of signal amplitude and noise variance from MR data. Magnetic Resonance in Medicine 51 (3), 586–594.

Smith, S.M., Brady, J.M., 1997. SUSAN – a new approach to low level image processing. International Journal of Computer Vision 23 (1), 45–78.

Tomasi, C., Manduchi, R., 1998. Bilateral filtering for gray and color images. In: Sixth International Conference on Computer Vision, pp. 839–846.

Wong, W., Chung, A., 2004. Trilateral filtering: a non-linear noise reduction technique for MRI. In: International Society for Magnetic Resonance in Medicine, p. 2218.

Wood, J.C., Johnson, K.M., 1999. Wavelet packet denoising of magnetic resonance images: importance of Rician noise at low SNR. Magnetic Resonance in Medicine 41, 631–635.

Yaroslavsky, L.P., 1985. Digital Picture Processing – An Introduction. Springer-Verlag.